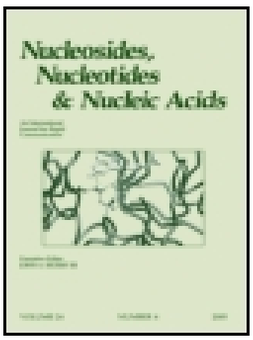

Nucleosides, Nucleotides and Nucleic Acids

ISSN: 1525-7770 (Print) 1532-2335 (Online) Journal homepage: http://www.tandfonline.com/loi/lncn20

Interactions of 4,4'-diaminoazobenzene derivatives with telomeric G-quadruplex DNA

Jeremy E. B. McCallum, Christopher W. Coyle, Ryan R. Elson & Blake A. Titterington

To cite this article: Jeremy E. B. McCallum, Christopher W. Coyle, Ryan R. Elson & Blake A. Titterington (2018): Interactions of 4,4′-diaminoazobenzene derivatives with telomeric G-quadruplex DNA, Nucleosides, Nucleotides and Nucleic Acids, DOI: 10.1080/15257770.2018.1442578

To link to this article: https://doi.org/10.1080/15257770.2018.1442578

Published online: 12 Mar 2018.

NUCLEOSIDES, NUCLEOTIDES AND NUCLEIC ACIDS
2018, VOL. 0, NO. 0, 1–10
https://doi.org/10.1080/15257770.2018.1442578

Taylor & Francis
Taylor & Francis Group

Interactions of 4,4′-diaminoazobenzene derivatives with telomeric G-quadruplex DNA

Jeremy E. B. McCallum[a], Christopher W. Coyle[b], Ryan R. Elson[a], and Blake A. Titterington[c]

[a]Department of Chemistry and Biochemistry, Loyola Marymount University, Los Angeles, CA, USA; [b]Molecular and Systems Pharmacology, Emory University, Atlanta, GA, USA; [c]School of Medicine, Creighton University, Omaha, NE, USA

ABSTRACT

The development of small molecules to stabilize the G-quadruplex structure has garnered significant attention for anticancer drug discovery. Herein, we report the synthesis of several 4,4′-diaminoazobenzene derivatives containing different substituent groups and their ability to bind and stabilize telomeric G-quadruplex DNA. Circular dichroism (CD) spectroscopy was performed to characterize the quadruplex topologies, measure stabilization effects, and evaluate their capabilities for conformational photoregulation. 4,4′-Diaminoazobenzene derivatives were found to moderately stabilize quadruplex structures but not affect conformational photoregulation. This work further develops the design and general understanding of the stabilization effects of small molecules with telomeric G-quadruplex DNA.

ARTICLE HISTORY
Received 1 July 2017
Revised 2 February 2018
Accepted 11 February 2018

KEYWORDS
G-quadruplexes; 4,4′-diaminoazobenzene; photoisomerization; circular dichroism

Introduction

G-quadruplexes are secondary structures formed in guanine-rich sequences of nucleic acids. G-tetrads, formed from the association of four guanine bases through Hoogsteen base pairing, coordinate with cations and stack on top of each other to form the quadruplex structure. These structures can assemble from one, two, or four nucleic acid strands, forming a variety of topologies that can be classified as parallel, antiparallel, and hybrid. The quadruplex structure can occur naturally in G-rich sequences and have been identified in telomeres and gene promoter regions. Proteins and ligands can bind G-quadruplexes, stabilizing the tertiary structure of DNA and RNA, and inhibit or promote replication, transcription, and translation.[1–4]

As these structures are linked to such diverse functions, the development of small molecules to stabilize the G-quadruplex structure for therapeutic purposes has garnered significant attention. Small molecule stabilization of quadruplex formation in

CONTACT Jeremy E. B. McCallum jeremy.mccallum@lmu.edu Department of Chemistry and Biochemistry, Loyola Marymount University, 1 LMU Drive, Los Angeles, CA, 90045, USA.
Color versions of one or more of the figures in the article can be found online at www.tandfonline.com/lncn.

telomeric DNA was one of the first targets as the G-quadruplex structure has been shown to decrease telomerase activity. Telomerase, which is responsible for maintaining the length of telomeres, is expressed in approximately 85% of cancer cells, providing inhibition as an attractive candidate for anticancer therapies.[5–7] Several quadruplex stabilizers such as telomestatin, RHPS4, and BRACO-19 have shown promising results.[8–10]

Our group is interested in developing small-molecule quadruplex stabilizers and targeted azobenzene derivatives for their photoregulation potential. Azobenzene derivatives can photoisomerize to the *cis* isomer under ultraviolet light and back to the *trans* isomer under visible light. Several 4,4′-dihydroxyazobenzene derivatives have been synthesized and shown to stabilize or destabilize the quadruplex structure dependent upon formation of the *trans* or *cis* isomer.[11–14] Derivatization of azoaniline moieties have not, as of yet, been investigated. We here report derivatization of 4,4′-diaminoazobenzene and the effect of several amino side chains on the stabilization of the DNA quadruplex structure.

Results and discussion

Synthesis

4,4′-Diaminoazobenzene (**1**) was synthesize by the sodium sulfide reduction of disperse orange 3 as previously described.[15] A one-pot preparation of diaminoazobenzene derivatives **2–7** (DAAB 2–7) was achieved upon treatment of 4,4′-diaminoazobenzene with the corresponding chloroacyl chloride (2-chloroacetyl chloride or 3-chloropropionyl chloride) followed by the addition of diethylamine, pyrrolidine, piperidine, or morpholine in moderate to good overall yields (Scheme 1).

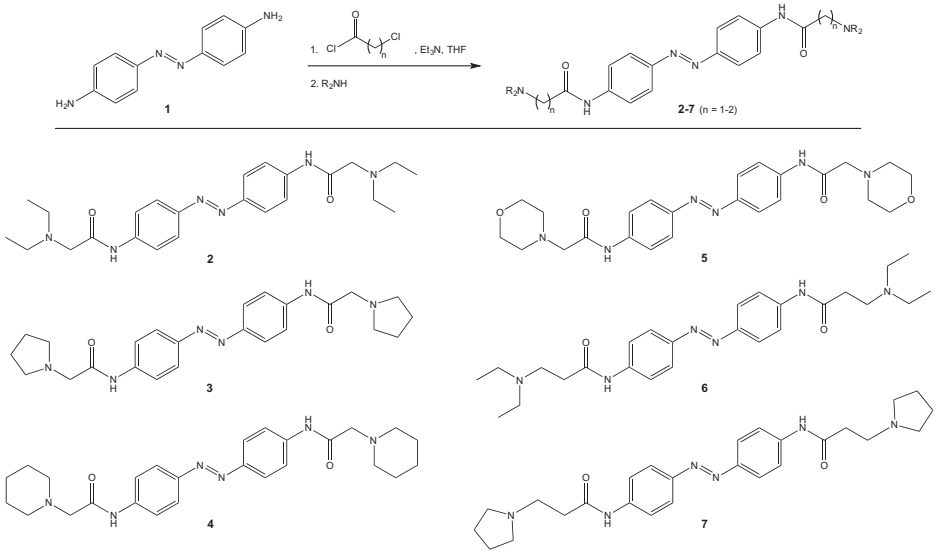

Scheme 1. Synthesis of 4,4′-diaminoazobenzene derivatives **2**–**7**.

CD spectroscopy

Telomeric DNA has been shown to be polymorphic, capable of forming several topologies with specific circular dichroism (CD) spectroscopic signatures. Parallel, anti-parallel, and hybrid quadruplex structures can be determined by specific positive and negative peaks within 180–300 nm range where DNA absorbs light.[16–18] Two DNA strands, **TEL6** (d(TTAGGG)) and **TEL24** (d(TTAGGG)$_4$), were found to form stable G-quadruplex structures in Tris-HCl-KCl buffer. The CD spectrum of **TEL6** showed a negative peak at 240 nm, a positive peak at 260 nm, and a weak negative peak at 284 nm characteristic of a parallel, tetramolecular G-quadruplex structure (Fig. 1a). The spectrum of **TEL24** exhibited a positive peak at 288 nm with a shoulder at 270 nm, indicative of a hybrid-type, monomolecular G-quadruplex (Fig. 1b). The CD spectrum of **TEL6** and **TEL24** in the presence of compound **7**

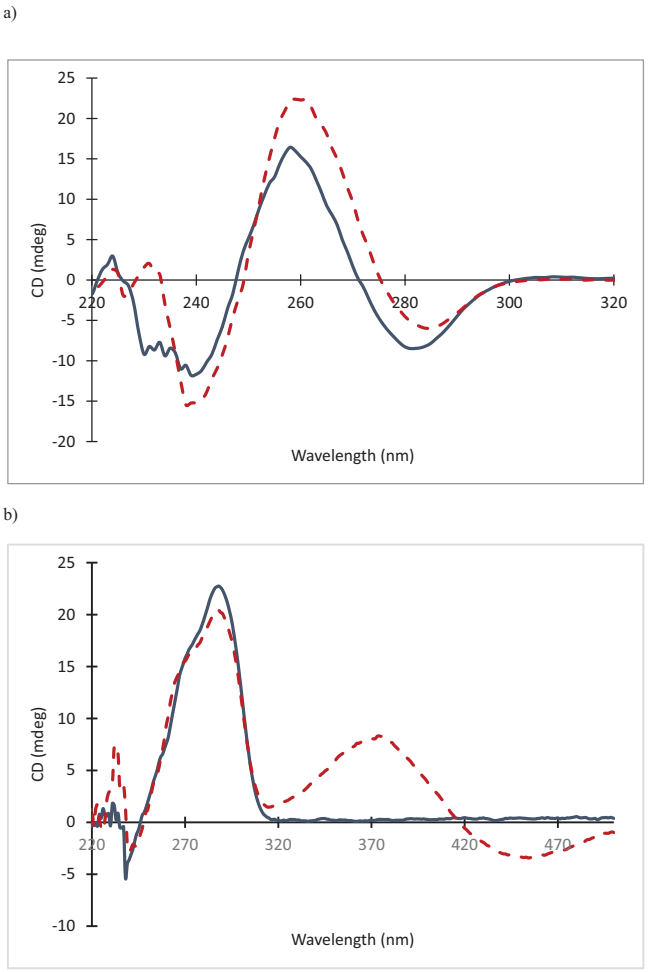

Figure 1. CD spectra of 10 μM telomeric quadruplex DNA in Tris-HCl-KCl buffer. The solid blue spectrum is quadruplex DNA without ligand while the red dashed spectrum contains compound **7** in a 4:1 ratio of ligand:[quadDNA]. a) CD spectra of **TEL6** in the presence and absence of compound **7**. b) CD spectra of **TEL24** in the presence and absence of compound **7**.

Table 1. Changes in melting curves of quadruplex DNA. $\Delta T_m = T_m$ (DNA+ligand) – T_m (DNA). Thermal melting of **TEL6** was monitored at 264 nm and **TEL24** was monitored at 288. The ratio represents [ligand]:[quadDNA].

	ΔT_m (°C)			
	TEL 6		TEL 24	
Compound	4:1	8:1	4:1	8:1
2	1.1	1.5	1.3	1.6
3	2.2	3.5	2.6	5.3
4	0.3	—	0.6	—
5	0.5	—	0.4	—
6	1.8	2.8	2.0	4.4
7	3.3	3.8	3.6	5.4

(consistent for compounds 2–6, data not shown) exhibited similar peaks, indicating the diaminoazobenzene derivatives formed the same topologies. Compound **7** (DAAB **7**) exhibited strong induced CD bands at 374 nm (positive) and 454 nm (negative) which confirm the interaction of **7** with the quadruplex DNA. Induced CD bands have been shown to aid in deciphering specific binding modes as end-stacking, intercalation, or groove-binding.[19–27] The bisignate shape in the visible range, containing one positive and one negative band, is suggestive of an exciton effect and indicative of the formation of dimer or higher order DAAB **7**-complexes associated with the quadruplex DNA.

Thermal stability studies

After confirming quadruplex formation, the quadruplex stabilization effects for each derivative were measured. Melting curve profiles were conducted for both **TEL6** and **TEL24** in the absence and presence of compounds **2–7** at two different concentrations. The changes in melting temperature (ΔT_m) of the quadruplex DNA were calculated and reported in Table 1.

4,4′-Diaminoazobenzene derivatives displayed minor to moderate quadruplex stabilization effects with greater ΔT_m temperatures for the hybrid G-quadruplex structure of **TEL24**. Not surprisingly, changing amino side chains affected quadruplex stabilization. Compounds **3** and **7**, both with pyrrolidinyl side chains, showed the largest stabilization effects for both quadruplex topologies. Compound to DNA ratios greater than 2:1 were required to see stabilization effects greater than 4°C, confirming the importance that dimer or higher-order DAAB derivative-complexes bound to DNA contribute to the observed stabilization effects.

Quadruplex DNA mobility assay

A native gel electrophoresis experiment (Figure 2) was performed to investigate the possibility of higher order (dimer, trimer) DNA quadruplex assemblies upon complexation with DAAB derivatives. **TEL24** migrated faster than the marker dyes (bromophenol blue, xylene cyanol) which respectively migrate to the same point as

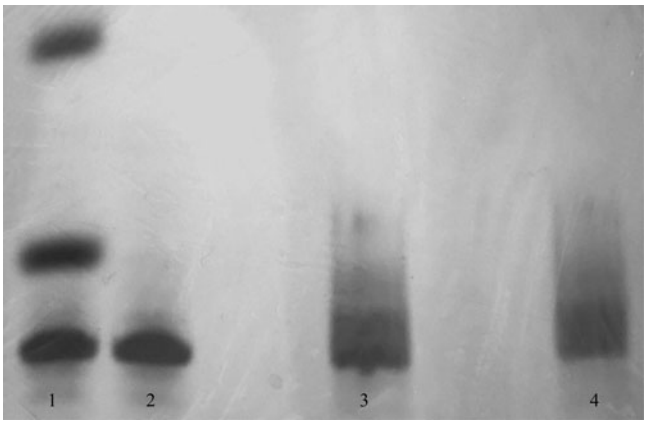

Figure 2. Native polyacrylamide gel electrophoresis of of compound 7 and **TEL24** DNA. Lane 1, **TEL24** with dye markers (bromophenol blue, xylene cyanol); lane 2, **TEL24**; lane 3, **TEL24** with 7 (1:4); lane 4, **TEL24** with 7 (1:8).

double-stranded DNA of 12 bp and 45 bp in a 20% polyacrylamide nondenaturing gel as previously demonstrated.[28–29] In the presence of compound **7**, **TEL24** predominantly migrated the same as the **TEL24** DNA alone. These results support that higher order DAAB-templated DNA assemblies (dimer, trimer, etc.) are not observed and that DAAB derivative-complexation occurs on single quadruplex monomer units.

Photoregulation

As the best stabilizer, compound **7** was chosen for evaluation of photoregulation of the quadruplex structure. When irradiated with light at 350 nm, compound **7** (in the presence of **TEL24**) photoisomerized from the *trans* to the *cis* isomer as indicated by changes in the UV/VIS spectrum and in agreement with previous

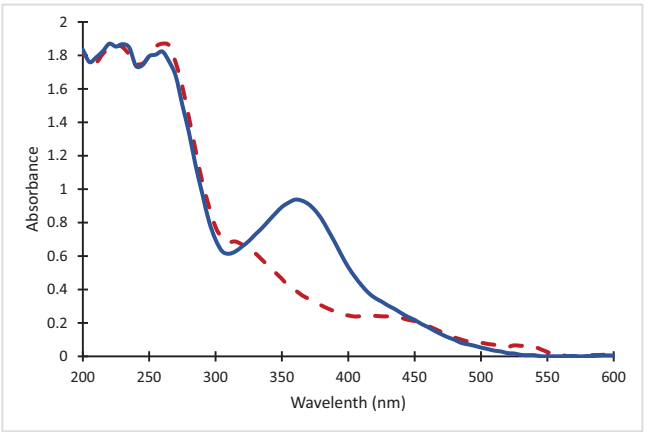

Figure 3. UV/Vis spectrum of compound **7** in **TEL24** DNA in Tris-HCl-KCl buffer. The solid blue line represents compound **7** before irradiation while the dashed red line represents compound **7** after 5 min irradiation.

work (Figure 3).[11–12,14] While the UV/VIS spectra demonstrated successful photoisomerization, no changes were observed in the CD spectrum below 300 nm as expected, indicating a lack of regulation (dissociation or conformation change) of the hybrid quadruplex conformation. As **TEL24** formed hybrid-type quadruplex structures in the presence and absence of compound **7**, a conformational change is not expected, assuming the *cis* isomer does not substantially bind DNA to induce a conformational change. Indeed Wang et al. and Xing et al. demonstrated relatively similar CD spectra for quadruplex DNA in the absence and presence of *cis*-4,4′-dihydroxyazobenzene derivatives while their *trans*-4,4′-dihydroxyazobenzene derivatives induced quadruplex DNA conformational changes.[11–12] In our case, the only change in CD spectra occurred for the induced CD bands which were diminished immediately after photoisomerization but returned to the same values within 5 minutes, indicating an initial reduction in higher order DAAB **7** to DNA complexation. Presumably, the *cis* isomer of **7** would decrease quadruplex DNA stabilization as compared to the *trans* isomer, resulting in a decreased ΔT_m, but isomerization back to the *trans* form occurs faster than the time in which the melting curve measurements can be completed.

Conclusions

Six 4,4-diaminoazobenzene derivatives were synthesized and found to bind to and stabilize quadruplex DNA. In the presence of **TEL6**, (d(TTAGGG)), parallel quadruplexes were formed while **TEL24**, ($d(TTAGGG)_4$), formed hybrid-type quadruplex structures. DNA stabilization effects were weak to moderate with the greatest effect demonstrated by compound **7** containing a pyrrolidinyl side chain, stabilizing the hybrid-type quadruplex most effectively. Induced CD bands indicated stabilization appeared to occur through a dimer or higher order complex associated with quadruplex DNA for TEL24. Photoisomerization from the *trans* to *cis* isomer had no apparent effect on the quadruplex conformation. This work further develops the design and general understanding of the stabilization effects of azobenzene derivatives with telomeric G-quadruplex DNA.

Experimental section

General information

All reagents were purchased from Aldrich Chemical Company and used without further purification. DNA was purchased from Integrated DNA Technologies with standard desalting purification and used without further purification. NMR spectra were recorded on a Bruker Avance-400 Spectrometer. Circular dichroism spectra were collected on a JASCO J-815 Circular Dichroism spectrophotometer using 0.1-cm path length quartz cuvettes. Electrospray ionization mass spectra were performed on an Agilent 6530 Q-TOF ESI mass spectrometer or a PerkinElmer Flexar SQ 300 ESI mass spectrometer. UV/Vis spectra were collected on an Agilent Cary

60 spectrophotometer. Photoirradiation was performed using a UVP, 5 watt UV lamp at 365 nm and maximum isomerization was achieved after 5 minutes. Automated column chromatography was achieved through flash chromatography using a CombiFlash® system.

Circular dichroism

A 40 μM solution [10 μM quadruplex] of **TEL6** (d(TTAGG) and 10 μM of **TEL24** ($d(TTAGGG)_4$ were prepared in 10 mM HCl-Trizma®base buffer solution with 100 mM KCl at a pH of 7.5. Stock solutions of compounds 2–7 were prepared in DMSO with final concentrations of 20 μM, 40 μM, and 80 μM for the corresponding studies. Full spectra scans (200 nm – 600 nm) were recorded at 25°C and melting curve profiles were performed at ramp rate of 1°C/min with a D.I.T. of 16 sec. and a band width of 2 nm.

Gel electrophoresis

Gel electrophoresis experiments were performed on a native gel containing 20% polyacrylamide (acrylamide/bis-acrylamide = 37.5:1) in TBE buffer. 40 mM KCl was added to the buffer and gel to maintain G-quadruplex structure formation. The gel was run at 4°C and viewed by UV shadowing.

Synthesis

4,4′-diaminoazobenzene (1)

8.66 g (0.036 mol) of $Na_2S{\cdot}9H_2O$ was solubilized in 300 mL of H_2O and added dropwise to a solution of 3.63 g of disperse orange 3 (0.015 mol) in 300 mL of MeOH over 1 hour. The resulting mixture was refluxed at 85°C for 3 hours. The product was precipitated in 600 mL of cold H_2O, vacuum filtered, and purified by automated flash chromatography (hexanes/ethyl acetate) to yield the final product in 87% yield.

^{1}H NMR (400 MHz; $CDCl_3$): δ 3.94 (br. s, 4H), 6.73 (d, $J = 8.2$ Hz, 4H), 7.73 (d, $J = 8.2$ Hz, 4H) ppm. ^{13}C NMR (100 MHz; $CDCl_3$): δ 114.9, 124.5, 146.0, 148.7 ppm. ESI-MS: Calcd for $C_{12}H_{13}N_4$ $[M+H]^+$ 213.11, found: 213.06.

General synthesis of compounds 2–7

0.425 g (0.002 mol) of 4,4′-diaminoazobenzene was dissolved in 100 mL of anhydrous THF and cooled with an ice bath. 1.2 mL (4 eq) of triethylamine and 3 eq. of the corresponding acid chloride was added sequentially. The reaction was warmed to room temperature and allowed to react for 2 hours. The reaction mixture was then cooled in an ice bath and 6 equivalents of the corresponding amine (pyrrolidine, diethylamine, piperidine, or morpholine) was added and stirred at room temperature overnight. After concentration, the crude product was dissolved in DCM and washed 3 times with an equal volume of saturated sodium bicarbonate solution.

The final product was purified using automated column flash chromatography (hexanes/ethyl acetate) to afford the final derivatives in good yields. For compounds 6–7, trimethylamine was omitted and 10 eq. of the corresponding amines were used.

N,N′-(diazene-1,2-diylbis(4,1-phenylene))bis(2-(diethylamino)acetamide) (2)

^{1}H NMR (400 MHz; $CDCl_3$): δ 1.11 (t, $J = 6.4$ Hz, 12H), 2.68 (q, $J = 6.4$ Hz, 8H), 3.18 (s, 4H), 7.73 (d, $J = 7.8$ Hz, 4H), 7.91 (d, $J = 7.8$ Hz, 4H), 9.53 (br. s, 2H) ppm. ^{13}C NMR (100 MHz; $CDCl_3$): δ 12.6, 49.1, 58.4, 119.5, 124.1, 140.2, 149.2, 170.5 ppm. ESI-MS: Calcd for $C_{24}H_{35}N_6O_2$ $[M+H]^+$ 439.28, found: 439.03. 62% yield.

N,N′-(diazene-1,2-diylbis(4,1-phenylene))bis(2-(pyrrolidin-1-yl)acetamide) (3)

^{1}H NMR (400 MHz; $CDCl_3$): δ 1.88 (br. s, 8H), 2.72 (br. s, 8H), 3.31 (s, 4H), 7.74 (d, $J = 7.6$ Hz, 4H), 7.91 (d, $J = 7.6$ Hz, 4H), 9.31 (br. s, 2H) ppm. ^{13}C NMR (100 MHz; $CDCl_3$): δ 24.3, 54.8, 60.0, 119.7, 124.0, 140.2, 149.2, 169.5 ppm. ESI-MS: Calcd for $C_{24}H_{31}N_6O_2$ $[M+H]^+$ 435.25, found: 435.13. 65% yield.

N,N′-(diazene-1,2-diylbis(4,1-phenylene))bis(2-(piperidin-1-yl)acetamide) (4)

^{1}H NMR (400 MHz; $CDCl_3$): δ 1.52 (br. s, 4H), 1.68 (br. s, 8H), 2.58 (br. s, 8H), 3.12 (s, 4H), 7.73 (d, $J = 7.6$ Hz, 4H), 7.92 (d, $J = 7.6$ Hz, 4H), 9.51 (br. s, 2H) ppm. ^{13}C NMR (100 MHz; $CDCl_3$): δ 23.7, 51.7, 55.1, 63.0, 119.6, 124.1, 140.2, 149.2, 169.2 ppm. ESI-MS: Calcd for $C_{24}H_{33}N_8O_2$ $[M+H]^+$ 463.28, found: 463.31. 60% yield.

N,N′-(diazene-1,2-diylbis(4,1-phenylene))bis(2-morpholinoacetamide) (5)

^{1}H NMR (400 MHz; $CDCl_3$): δ 2.65 (br. s, 8H), 3.18 (s, 4H), 3.80 (br. s, 8H), 7.73 (d, $J = 8.0$ Hz, 4H), 7.92 (d, $J = 8.0$ Hz, 4H), 9.26 (br. s, 2H) ppm. ^{13}C NMR (100 MHz; $CDCl_3$): δ 54.0, 62.7, 67.2, 119.7, 124.1, 139.9, 149.3, 168.2 ppm. ESI-MS: Calcd for $C_{24}H_{31}N_6O_4$ $[M+H]^+$ 467.24, found: 467.20. 57% yield.

N,N′-(diazene-1,2-diylbis(4,1-phenylene))bis(3-(diethylamino)propanamide) (6)

^{1}H NMR (400 MHz; $CDCl_3$): δ 1.14 (t, $J = 6.8$ Hz, 12H), 2.53 (t, $J = 6.7$ Hz, 4H), 2.69 (q, $J = 6.8$ Hz, 8H), 2.79 (t, $J = 6.7$ Hz, 4H), 7.77 (d, $J = 7.8$ Hz, 4H), 7.88 (d, $J = 7.8$ Hz, 4H), 11.62 (br. s, 2H) ppm. ^{13}C NMR (100 MHz; $CDCl_3$): δ 11.6, 33.3, 46.1, 49.0, 119.6, 124.0, 141.3, 148.8, 171.3 ppm. ESI-MS: Calcd for $C_{24}H_{35}N_6O_2$ $[M+H]^+$ 467.3, found: 467.2. 42% yield

N,N′-(diazene-1,2-diylbis(4,1-phenylene))bis(3-(pyrrolidin-1-yl)propanamide) (7)

^{1}H NMR (400 MHz; $CDCl_3$): δ 1.88 (br. s, 8H), 2.53 (t, $J = 6.7$ Hz, 4H), 2.72 (br. s, 8H), 2.79 (t, $J = 6.7$ Hz, 4H), 7.74 (d, $J = 7.6$ Hz, 4H), 7.91 (d, $J = 7.6$ Hz, 4H), 11.62 (br. s, 2H) ppm. ^{13}C NMR (100 MHz; $CDCl_3$): δ 24.3, 33.0, 54.8, 56.0, 119.7, 124.0, 140.2, 149.2, 171.5 ppm. ESI-MS: Calcd for $C_{24}H_{31}N_6O_2$ $[M+H]^+$ 463.3, found: 463.1. 38% yield.

References

[1] Viglasky, V.; Hianik, T. Potential uses of G-quadruplex-forming aptamers. *Gen. Physiol. Biophys.* **2013**, *32* (2), 149–172.

[2] Simonsson, T. G-quadruplex DNA structures – Variations on a theme. *Biol. Chem.* **2001**, *382* (4), 621–628.

[3] Dolinnaya, N. G.; Ogloblina, A. M.; Yakubovskaya, M. G. Structure, properties, and biological relevance of the DNA and RNA G-quadruplexes: Overview 50 years after their discovery. *Biochemistry (Moscow)* **2016**, *81* (13), 1602–1649.

[4] Collie, G. W.; Parkinson, G. N. The application of DNA and RNA G-quadruplexes to therapeutic medicines. *Chem. Soc. Rev.* **2011**, *40* (12), 5867–5892.

[5] Kim, N. W.; Piatyszek, M. A.; Prowse, K. R.; Harley, C. B.; West, M. D.; Ho, P. L. C.; Coviello, G. M.; Wright, W. E.; Weinrich, S. L.; Shay, J. W. Specific association of human telomerase activity with immortal cells and cancer. *Science* **1994**, *266* (5193), 2011–2015.

[6] Perry, P. J.; Reszka, A. P.; Wood, A. A.; Read, M. A.; Gowan, S. M.; Dosanjh, H. S.; Trent, J. O.; Jenkins, T. C.; Kelland, L. R.; Neidle, S. Human telomerase inhibition by regioisomeric disubstituted amidoanthracene-9,10-diones. *J. Med. Chem.* **1998**, *41* (24), 4873–4884.

[7] Fedoroff, O. Y.; Salazar, M.; Han, H. Y.; Chemeris, V. V.; Kerwin, S. M.; Hurley, L. H. NMR-based model of a telomerase-inhibiting compound bound to G-quadruplex DNA. *Biochemistry* **1998**, *37* (36), 12367–12374.

[8] Xu, Y. C.; Goldkorn, A. Telomere and Telomerase Therapeutics in Cancer. *Genes* **2016**, *7* (6), 22.

[9] Gomez, D. L. M.; Armando, R. G.; Cerrudo, C. S.; Ghiringhelli, P. D.; Gomez, D. E. Telomerase as a Cancer Target. Development of New Molecules. *Curr. Top. Med. Chem.* **2016**, *16* (22), 2432–2440.

[10] Buseman, C. M.; Wright, W. E.; Shay, J. W. Is telomerase a viable target in cancer? *Mutat. Res.* **2012**, *730* (1–2), 90–97.

[11] Wang, X. L.; Huang, J.; Zhou, Y. Y.; Yan, S. Y.; Weng, X. C.; Wu, X. J.; Deng, M. G.; Zhou, X. A. Conformational Switching of G-Quadruplex DNA by Photoregulation. *Angew. Chem. Int. Ed.* **2010**, *49* (31), 5305–5309.

[12] Xing, X. W.; Wang, X. L.; Xu, L.; Tai, Y.; Dai, L. Y.; Zheng, X. L.; Mao, W. X.; Xu, X. W.; Zhou, X. Light-driven conformational regulation of human telomeric G-quadruplex DNA in physiological conditions. *Org. Biomol. Chem.* **2011**, *9* (19), 6639–6645.

[13] Tian, T.; Song, Y. Y.; Wang, J. Q.; Fu, B. S.; He, Z. Y.; Xu, X. Q.; Li, A. L.; Zhou, X.; Wang, S. R. Small-Molecule-Triggered and Light-Controlled Reversible Regulation of Enzymatic Activity. *J. Am. Chem. Soc.* **2016**, *138* (3), 955–961.

[14] Thevarpadam, J.; Bessi, I.; Binas, O.; Goncalves, D. P. N.; Slavov, C.; Jonker, H. R. A.; Richter, C.; Wachtveitl, J.; Schwalbe, H.; Heckel, A. Photoresponsive Formation of an Intermolecular Minimal G-Quadruplex Motif. *Angew. Chem. Int. Ed.* **2016**, *55* (8), 2738–2742.

[15] Kanie, K.; Nishii, M.; Yasuda, T.; Taki, T.; Ujiie, S.; Kato, T. Self-assembly of thermotropic liquid-crystalline folic acid derivatives: hydrogen-bonded complexes forming layers and columns. *J. Mater. Chem.* **2001**, *11* (11), 2875–2886.

[16] Prislan, I.; Lah, J.; Vesnaver, G. Diverse Polymorphism of G-Quadruplexes as a Kinetic Phenomenon. *J. Am. Chem. Soc.* **2008**, *130* (43), 14161–14169.

[17] Burge, S.; Parkinson, G. N.; Hazel, P.; Todd, A. K.; Neidle, S. Quadruplex DNA: sequence, topology and structure. *Nucleic Acids Res.* **2006**, *34* (19), 5402–5415.

[18] Borovok, N.; Iram, N.; Zikich, D.; Ghabboun, J.; Livshits, G. I.; Porath, D.; Kotlyar, A. B. Assembling of G-strands into novel tetra-molecular parallel G4-DNA nanostructures using avidinbiotin recognition. *Nucleic Acids Res.* **2008**, *36* (15), 5050–5060.

[19] Chen, Q.; Kuntz, I. D.; Shafer, R. H. Spectroscopic recognition of guanine dimeric hairpin quadruplexes by a carbocyanine dye. *PNAS* **1996**, *93* (7), 2635–2639.

[20] Rodger, A.; Taylor, S.; Adlam, G.; Blagbrough, I. S.; Haworth, I. S. Multiple DNA-Binding Modes of Anthracene-9-Carbonyl-N-1 Spermine. *Bioorg. Med. Chem.* **1995**, *3* (6), 861–872.
[21] Norden, B.; Tjerneld, F. Structure of Methylene-Blue DNA Complexes Studied by Linear and Circular-Dichroism Spectroscopy. *Biopolymers* **1982**, *21* (9), 1713–1734.
[22] Garbett, N. C.; Ragazzon, P. A.; Chaires, J. B. Circular dichroism to determine binding mode and affinity of ligand-DNA interactions. *Nat. Protoc.* **2007**, *2* (12), 3166–3172.
[23] Bai, L. P.; Hagihara, M.; Jiang, Z. H.; Nakatani, K. Ligand Binding to Tandem G Quadruplexes from Human Telomeric DNA. *ChemBioChem.* **2008**, *9* (16), 2583–2587.
[24] Zhang, W.; Chen, M.; Wu, Y. L.; Tanaka, Y.; Ji, Y. J.; Zhang, S. L.; Wei, C. H.; Xu, Y. Formation and stabilization of the telomeric antiparallel G-quadruplex and inhibition of telomerase by novel benzothioxanthene derivatives with anti-tumor activity. *Sci. Rep.* **2015**, *5*, 13693.
[25] Hudson, J. S.; Brooks, S. C.; Graves, D. E. Interactions of Actinomycin D with Human Telomeric G-Quadruplex DNA. *Biochemistry* **2009**, *48* (21), 4440–4447.
[26] Bhadra, K.; Kumar, G. S. Interaction of berberine, palmatine, coralyne, and sanguinarine to quadruplex DNA: A comparative spectroscopic and calorimetric study. *Biochim. Biophys. Acta.* **2011**, *1810* (4), 485–496.
[27] White, E. W. *Selective Recognition of Quadruplex DNA by Small Molecules*; Georgia State University: Atlanta, GA, **2006**.
[28] Kim, M.Y.; Gleason-Guzman, M.; Izbicka, E.; Nishioka, D.; Hurley, L. H. The different biological effects of telomestatin and TMPyP4 can be attributed to their selectivity for interaction with intramolecular or intermolecular G-quadruplex structures. *Cancer Res.* **2003**, *63*, 3247–3256.
[29] Sambrook, J.; Fritsch, E.F.; Maniatis, T. *Molecular Cloning: A Laboratory Manual*, 2nd ed., Cold Spring Harbor Laboratory, Cold Spring Harbor, **1989**.